metals

MDPI

Article

Corrosion of Molybdenum-Based and Ni–Mo Alloys in Liquid Bismuth–Lithium Alloy

Aleksander V. Abramov [1,*], Ruslan R. Alimgulov [2], Anastasia I. Trubcheninova [2], Arkadiy Yu. Zhilyakov [3], Sergey V. Belikov [3], Vladimir A. Volkovich [2] and Ilya B. Polovov [2]

[1] Department of Physical and Chemical Methods of Analysis, Ural Federal University, 620002 Ekaterinburg, Russia
[2] Department of Rare Metals and Nanomaterials, Ural Federal University, 620002 Ekaterinburg, Russia
[3] Department of Heat Treatment and Physics of Metals, Ural Federal University, 620002 Ekaterinburg, Russia
* Correspondence: abramov.urfu@mail.ru

Abstract: Bismuth–lithium alloys are considered primary candidates for the reductive extraction step in the on-line reprocessing of molten salt reactor fuel. The corrosion behavior of molybdenum-based alloys and Hastelloy® B-3 alloy (taken for comparison) was examined here in a liquid Bi–Li (5 mol.%) alloy at 650 °C. MoW10, MoW30, and TZM corrosion-resistant alloys were studied as prospective construction materials for holding liquid bismuth–lithium alloy. Rates of corrosion were determined by the gravimetric method as well as by chemical analysis of corrosion products formed in liquid-phase Bi–Li alloy. The microstructure and chemical composition of samples of the materials and Bi–Li alloys containing the corrosion products after the tests were determined using inductively coupled plasma–atomic emission spectroscopy, X-ray fluorescence analysis, scanning electron microscopy, and energy dispersive spectroscopy. TZM molybdenum-based alloy corrodes in the bismuth-lithium alloy due to the formation of a zirconium–bismuth intermetallic compound, which passes into the liquid phase. The corrosion rates of MoW10, MoW30, and TZM alloys at 650 °C were 16, 16, and 23 μm/year, respectively. Hastelloy® B-3 alloy, despite its high molybdenum content, was subjected to severe corrosion in liquid Bi–Li alloys due to dissolution of nickel in liquid bismuth. The corrosion rate of this alloy was 14 mm/year.

Keywords: corrosion; bismuth; lithium; molybdenum; tungsten; zirconium; nickel; alloy

check for updates

Citation: Abramov, A.V.; Alimgulov, R.R.; Trubcheninova, A.I.; Zhilyakov, A.Y.; Belikov, S.V.; Volkovich, V.A.; Polovov, I.B. Corrosion of Molybdenum-Based and Ni–Mo Alloys in Liquid Bismuth–Lithium Alloy. *Metals* **2023**, *13*, 366. https://doi.org/10.3390/met13020366

Academic Editor: Changdong Gu

Received: 23 January 2023
Revised: 8 February 2023
Accepted: 9 February 2023
Published: 11 February 2023

Copyright: © 2023 by the authors. Licensee MDPI, Basel, Switzerland. This article is an open access article distributed under the terms and conditions of the Creative Commons Attribution (CC BY) license (https://creativecommons.org/licenses/by/4.0/).

1. Introduction

Liquid metal systems exhibit a range of unique properties that make them attractive for application in various key nuclear power technologies. Liquid lead–bismuth-based alloy is the primary coolant candidate in compact high-temperature reactors and fast neutron reactors [1]. Liquid bismuth–lithium alloy (5 mol.% Li) is of interest for prospective pyrochemical technologies in spent nuclear fuel (SNF) reprocessing. Reductive extraction of d- and f-elements on bismuth in the presence of lithium is currently widely studied as one of the stages in molten fluoride SNF reprocessing [2]. The practical implication of such extraction processes requires selecting construction materials with sufficient corrosion resistance in a "liquid bismuth–lithium alloy–fluoride melt" system.

The primary attention of research groups devoted to studying corrosion properties of construction materials in liquid metal media is focused on experiments related to the corrosion of various types of steels in liquid lead or bismuth–lead eutectic alloy. Primary causes of corrosion degradation of materials and ways of minimizing the impact of corrosion in these media can be transferred to bismuth–lithium alloys with one assumption, i.e., the corrosion activity of pure bismuth is 40 times higher than that of lead [3]. Analysis of previous studies allows us to make the following recommendation: To avoid dissolution of steels in liquid lead, it is necessary to keep oxygen concentration at a certain level (10^{-6}–10^{-7} at. %)

to form protective oxide layers. Such oxygen content in the liquid metal is sufficient for passivating materials but is not high enough to cause lead oxide precipitation. For steels, the minimum concentration of oxygen is determined by the potential of magnetite's (Fe_3O_4) decomposition, because this oxide is the least stable oxide phase that can be formed on construction steels. After the oxide layers are formed, the dissolution of construction materials becomes negligible due to low rates of diffusion of steel alloying components in oxides. An ideal protective oxide layer must be free of pores, cracks, and stresses at working temperatures, and must be resistant to chipping or damage upon cooling or heating [4]. In addition, oxygen and metal ions should have low diffusion coefficients in the oxide layer, and the rate of the oxide film dissolution must be sufficiently low during the entire period of exploitation [5]. In practice, under real conditions, it is essentially impossible to create such an ideal protective layer. However, it is possible to make a self-restoring layer by controlling oxygen concentration in liquid lead or lead–bismuth alloy as well as by varying steel composition and working conditions.

Application of such a mechanism for protecting construction materials used in the bismuth–lithium alloy extraction step is difficult due to the presence of molten fluoride salt in contact with the bismuth–lithium alloy. Fluoride melt is a powerful corrosion medium and easily dissolves oxide layers. Molybdenum and nickel alloys constitute prospective materials for work with fluoride melts. Previously [6], we tested pure metals (Mo and Ta) and several nickel alloys in liquid bismuth–lithium alloy. Nickel alloys showed severe corrosion degradation, but the corrosion of individual molybdenum and tantalum was insignificant. As a result, we decided to study the corrosion resistance of molybdenum alloys. Available literature data on the corrosion of molybdenum and its alloys in liquid bismuth are rather limited; there are several works devoted to studying corrosion processes in a bismuth–lead alloy and pure lead. Rivai et al. [7] investigated the corrosion behavior of some refractory metals (W, Mo, and Nb) in bismuth–lead eutectic alloy (LBE) at 700 °C. They reported that tungsten and molybdenum exhibited high corrosion resistance in the bismuth–lead eutectic alloy; there were no signs of penetration of the alloy components into the microstructure of the metals. Xiao et al. [8] held Mo–0.5La alloy in pure liquid lead at 1000 °C for 1000 h. They found that although the alloy in general showed high corrosion resistance, there were localized zones of etching on the surface of the samples.

The present work was aimed at studying the corrosion resistance of molybdenum-based alloys (MoW10, MoW30, TZM) and Hastelloy® B-3 alloy in liquid Bi–Li alloy. Hastelloy® B-3 alloy is a nickel–molybdenum alloy that was selected for the comparison of corrosion behavior and resistance with molybdenum-based alloys. During the reductive extraction step, the construction materials make contact with both liquid Bi–Li alloy and molten fluoride salt; the choice of the objects for the present study reflects this circumstance. Previously [6], we showed that molybdenum had high corrosion stability in fluoride melts and liquid Bi–Li alloy. Therefore, molybdenum-based alloys were now selected to assess their corrosion behavior in a Bi–Li alloy.

Past studies of the corrosion resistance of structural materials in contact with liquid metals showed that of all low-melting metals commonly used as coolants or heat carriers (i.e., Li, Na, Pb, Bi), bismuth was the most corrosive [9]. Possible intermetallic compounds (IMCs) than can be formed by bismuth with the principal elements present in the structural materials are listed in Table 1 [10].

Molybdenum and tungsten do not form IMCs with bismuth. The solubility of molybdenum in liquid bismuth does not exceed 10^{-4} wt. % at 1030 °C [11], and tungsten content in liquid bismuth after 120 h of contact at 778 °C was below 10^{-5} wt. % [12].

Zirconium is the component of TZM alloy, and this element is capable of forming five intermetallic compounds with bismuth through peritectic reactions (Table 1). Therefore, it was of considerable interest to study the corrosion resistance of TZM alloy in a Bi–Li melt.

Table 1. Solubility of metals in bismuth and possible intermetallic compounds formed in the corresponding binary systems.

Element	Fe	Ni	Mo	W	Al	Ti	Nb	Cr	Cu	Mn	Si	Zr
Solubility, at. % (at T, °C)	0.03 (650)	14, 35 (477, 1000)	0.003 (700)	0.00001 (778)	0.55–88.2 (678)	none	0.041 (750)	0.0036 (482–1000)	none	0.42 (265)	none	1.4 (700)
IMC	none	BiNi Bi_3Ni	none	none	none	Ti_3Bi Ti_2Bi	none	none	None	MnBi	none	$ZrBi_2$ ZrBi Zr_3Bi_2 Zr_3Bi Zr_3Bi

2. Materials and Methods

2.1. Materials

Samples of nickel-based alloys were cut from sheets (4 mm thick) and were of a rectangular shape. Samples of molybdenum-based alloys were cut from bars (10 mm diameter) and had the shape of cylinders 4 mm high. Preparation of the samples for the corrosion tests is described in detail elsewhere [6]. Composition of the alloys (in as-received state) is listed in Table 2.

Table 2. Composition of studied alloys according to the manufacturers' certificates, wt. %.

Alloy	Al	C	Cr	Fe	Mn	Mo	N	Ni	O	Si	Ti	W	Zr
MoW10		0.0023		0.0011		base	0.0020	0.0004	0.0033	0.0009		9.9	
MoW30		0.0024		0.0013		base	0.0020	0.0006	0.0033	0.0009		29.9	
TZM		0.01–0.04				base	—	—	—		0.45–0.55		0.06–0.12
Hastelloy® B-3 Alloy	0.33	0.002	1.63	1.41	0.68	28.50	—	base	—	0.04	<0.01	0.24	<0.01

Metallic bismuth (KITE METALS SARL, Windhof, Luxembourg) was of 99.99% purity. According to the manufacturer's specification, the main impurities were Ag (0.0012 wt. %), Pb (0.0003 wt. %), As (0.0002 wt. %), and Cu, Fe, Sb, and Zn (0.0001 wt. % each). X-ray fluorescence analysis (XRF) of bismuth showed a silver content of 0.0013 wt. %; all other impurities were below 0.001 wt. %. Lithium (99.9%) contained 0.01 wt. % Na, 0.03 wt. % Ca, 0.02 wt. % Mg, and 0.005 wt. % K and Fe (according to the manufacturers' certificate).

2.2. Corrosion Tests

The corrosion tests were carried out employing a custom-built setup for high-temperature corrosion studies described in detail in an earlier work [13]. This setup allows for the performing of long-term corrosion tests in various working media at elevated temperatures. A stream of gas or a gas mixture can be continuously passed through the experimental cells if required. The experiments were performed in the following manner: Three samples of a selected alloy material were used in each test. The samples were placed in low-porosity graphite crucibles, granules of metallic bismuth were loaded on top, and then the required amount of lithium was added to achieve the molar ratio of lithium to bismuth of 1:19 (corresponding to 0.17 wt. % Li in the liquid alloy phase).

Each crucible was covered by a graphite lid and placed in a steel cell that could be tightly closed using steel lids. Metallic titanium sponge was positioned in a holder in the upper part of the cell to act as a getter for additional purification of the atmosphere from possible oxygen impurities. The experimental setup used for the corrosion studies is schematically shown in Figure 1.

Each cell was sealed, evacuated, filled with argon, and placed in a vertical tube furnace. A flow of high-purity argon (99.999%) through the cell was maintained for the duration of the experiments. Argon was passed through the upper part of the cell at ca. 50 mL/min flow rate. Bismuth and lithium were loaded separately rather than as a fused mixture because these metals have low melting points (271.4 and 180.5 °C, respectively) and, therefore,

would fuse readily while the experimental cell is heated to the working temperature of 650 °C. The calls were heated at a 30 °C/mit rate and in less than 15 min, bismuth and lithium formed a liquid homogeneous alloy in the crucibles. High boiling points of lithium and bismuth (well in excess of 1000 °C) and lids on the crucibles prevented changes in the composition of Bi–Li alloy due to possible evaporation during fusing. After the cells were heated to 650 °C (the temperature in each cell was controlled by a thermocouple positioned inside in close proximity to the crucible, Figure 1), the cells were held at the working temperature for 100 h.

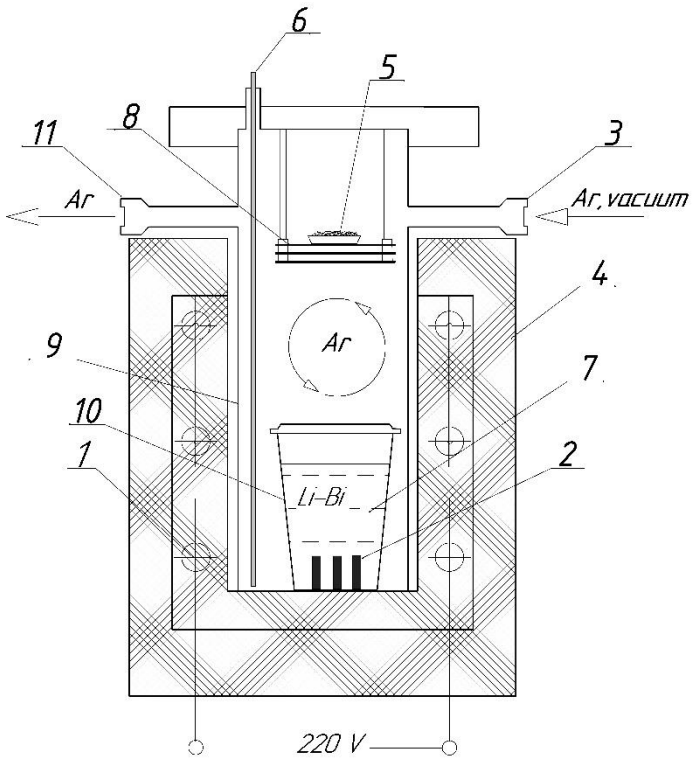


Figure 1. Experimental setup for corrosion experiments: heaters (**1**); test sample (**2**); gas inlet (**3**); furnace (**4**); titanium getter (**5**); thermocouple (**6**); liquid metal (**7**); nickel heat-reflecting screens (**8**); steel cell (**9**); crucible (**10**); gas outlet (**11**).

After completing the experiment, the cells were cooled to room temperature, opened, and the crucibles with the samples were taken out. Samples of the tested molybdenum and nickel alloys were separated from Bi–Li alloy, thoroughly washed, and dried. After measuring weight loss, the specimens were mounted in phenol hot-mounting resin with carbon filler for the subsequent metallographic analysis. Mounted samples were first sandpapered in six stages (SiC papers in the following order of grades: 80 → 220 → 320 → 1200 → 2400 → 4000). Finally, the samples were polished using a water-based diamond suspension (monocrystalline diamonds with a grain size of 1 μm, DiADuo-2, Struers) followed by a colloidal silica polishing suspension (OP-S, Struers).

The surface of the corroded samples was examined by scanning electron microscopy (SEM, JEOL JSM 6490, JEOL Ltd., Tokyo, Japan) with energy dispersive X-ray microanalysis (EDS, Oxford Inca, Oxford Inc., Oxford, UK) and SEM (ThermoFisher Scios 2, TermoFisher Scientifc Inc., Hilsboro, OR, USA) with a microanalysis attachment (Inka Energy TEM 350).

Bismuth–lithium alloys (BLA) after the corrosion tests were analyzed by XRF (ARL Advant'X 4200, TermoFisher Scientifc Inc., Hilsboro, OR, USA) and inductively coupled plasma–atomic emission spectroscopy (ICP–AES, Optima 2100 DV, PerkinElmer Inc., Waltham, MA, USA) to determine the content of impurities and the corrosion products.

3. Results and Discussion

Samples of the alloys prior to and after the corrosion tests in BLA are presented and compared in Figure 2. Hastelloy® B-3 alloy (Figure 2A) showed signs of severe corrosion, while molybdenum-based alloys (Figure 2B–D) showed very little change.

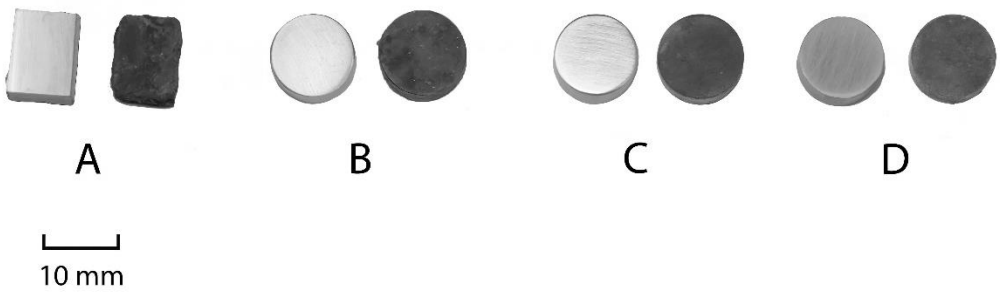


Figure 2. Appearance of the alloys before (left images) and after (right images) contact with Bi–Li alloy at 650 °C for 100 h: Hastelloy® B-3 Alloy (**A**); TZM (**B**); MoW10 (**C**); MoW30 (**D**).

Each sample was weighted prior to and after the corrosion test. Weight loss of the samples was used to calculate the corrosion rates in Bi–Li alloys (gravimetric method). Additionally, the corrosion rates for the alloys were calculated from the content of corrosion products in Bi–Li alloy after contact with tested materials (analytical method). Concentrations of the corrosion products of the alloy materials in Bi–Li alloy were determined by ICP–AES and XRF analyses, and the results are summarized in Table 3. Two analytical methods used for analyzing Bi–Li alloys showed satisfactory agreement regarding the results obtained.

Table 3. Content of the corrosion products in Bi–Li alloys after 100 h contact with Mo- and Ni-based alloys at 650 °C.

Alloy	Element	Corrosion Product Content (wt. %) Determined by	
		XRF	ICP–AES
MoW10	Mo	0.0005	0.0002
	W	<0.001	<0.0001
MoW30	Mo	0.0005	0.0002
	W	<0.001	<0.0001
TZM	Mo	0.001	0.0009
	Zr	<0.001	<0.0001
	Ti	<0.001	<0.0001
Hastelloy® B-3 Alloy	Ni	0.41	0.45
	Mo	<0.001	0.001
	Cr	<0.001	<0.001
	Fe	<0.001	<0.001

The corrosion rates determined by gravimetric and analytical methods are summarized in Table 4. For the analytical method, the results obtained using XRF and ICP–AES analyses are presented separately. The corrosion rates of Hastelloy® B-3 alloy could not be estimated using the gravimetric method since a significant amount of bismuth remained on the surface and in the bulk of the alloy samples.

The corrosion rates of molybdenum alloys were significantly lower than the rate of corrosion of the nickel–molybdenum alloy Hastelloy® B-3, the difference being around three orders of magnitude. Molybdenum–tungsten alloys showed the lowest corrosion rates, not exceeding 16 μm/year. Therefore, these alloys can be considered as prospective construction materials for applications in liquid Bi–Li alloys. The rate of corrosion of TZM

alloy was higher than that of MoW10 and MoW30 by ca. 30%. The increased corrosion rate could result from the formation of intermetallic compounds between zirconium and bismuth. However, zirconium content in BLA did not exceed 0.5 wt. % and no considerable corrosion of TZM alloy was observed. Nevertheless, this alloy is less attractive as a construction material than molybdenum–tungsten alloys.

Table 4. Corrosion rates of molybdenum- and nickel-based alloys in liquid Bi–Li (5 mol.%) alloys determined by various methods after 100 h contact at 650 °C.

System	Corrosion Rate (mm/Year) According to		
	Sample's Weight Loss	XRF Analysis	ICP–AES Analysis
MoW10	0.013 ± 0.003	0.014 ± 0.002	0.016 ± 0.002
MoW30	0.012 ± 0.002	0.015 ± 0.002	0.016 ± 0.001
TZM	0.018 ± 0.002	0.019 ± 0.002	0.023 ± 0.002
Hastelloy® B-3 Alloy	–	13.3 ± 0.3	14.2 ± 0.2

Nickel–molybdenum alloy Hastelloy® B-3 alloy showed very low stability and high corrosion rates in liquid Bi–Li alloy despite its high molybdenum content. Therefore, Hastelloy® B-3 alloy cannot be used as a construction material in liquid BLA media.

After contact with liquid BLA, samples of the alloys were examined by SEM to determine the possible nature of the alloys' surface degradation (Figures 3–5). The results revealed no significant changes in the microstructure of MoW10, MoW30, and TZM alloys; the surface was uniform with no significant damage.

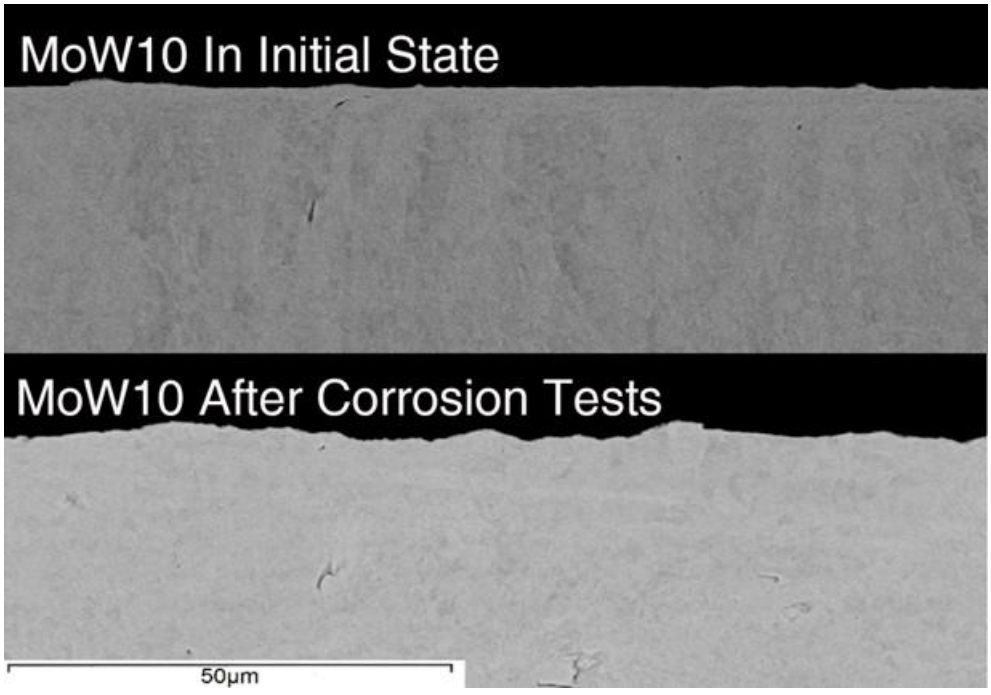


Figure 3. BSE-SEM images of microstructure of MoW10 alloy samples before and after contact with BLA at 650 °C for 100 h.

The high purity of BLA allowed us to exclude possible chemical interactions of impurities with Mo–W alloys. The major impurity in bismuth was silver (0.0012 wt. %), which does not form intermetallic compounds with tungsten or molybdenum [14–16] and, therefore, cannot influence the process of dissolution of these metals in Bi–Li alloys. Thus, the composition of BLA after the corrosion tests and analysis of the samples' surface allowed us to conclude that the corrosion rates of molybdenum alloys were determined

by the dissolution of these materials in bismuth. Such a conclusion is supported by the literature data [10–12,17] and the results obtained in an earlier work [6]. The solubility of molybdenum in bismuth is low and, at 700 °C, equals to 0.003 at. % or 0.0014 wt. % (Table 1). The results obtained here at 650 °C were of the same order; molybdenum concentration in BLA after the corrosion tests was 0.0005–0.001 wt. % (Table 3).

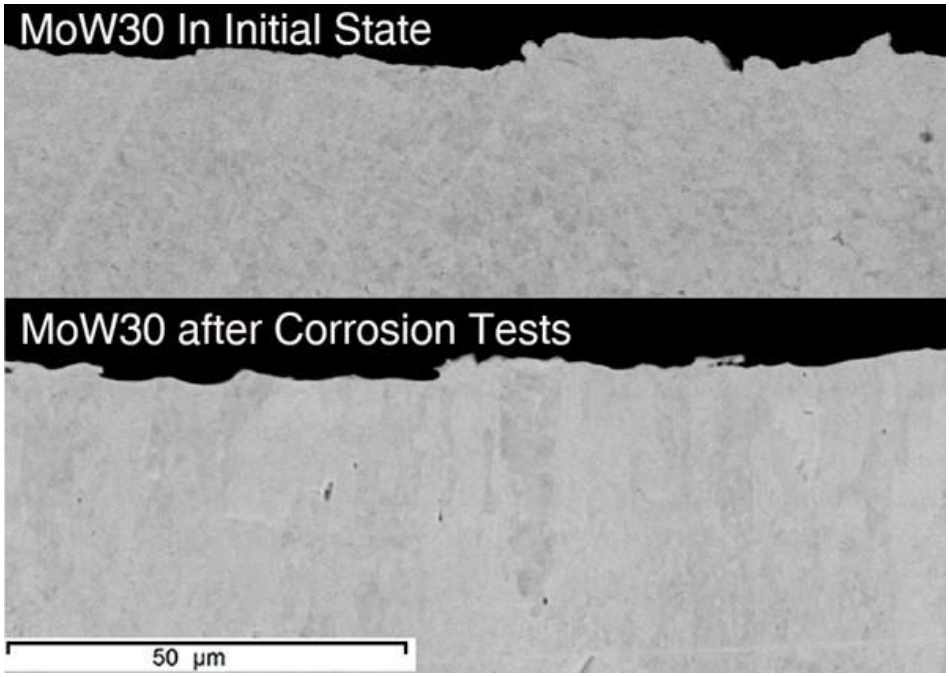


Figure 4. BSE-SEM images of microstructure of MoW30 alloy samples before and after contact with BLA at 650 °C for 100 h.

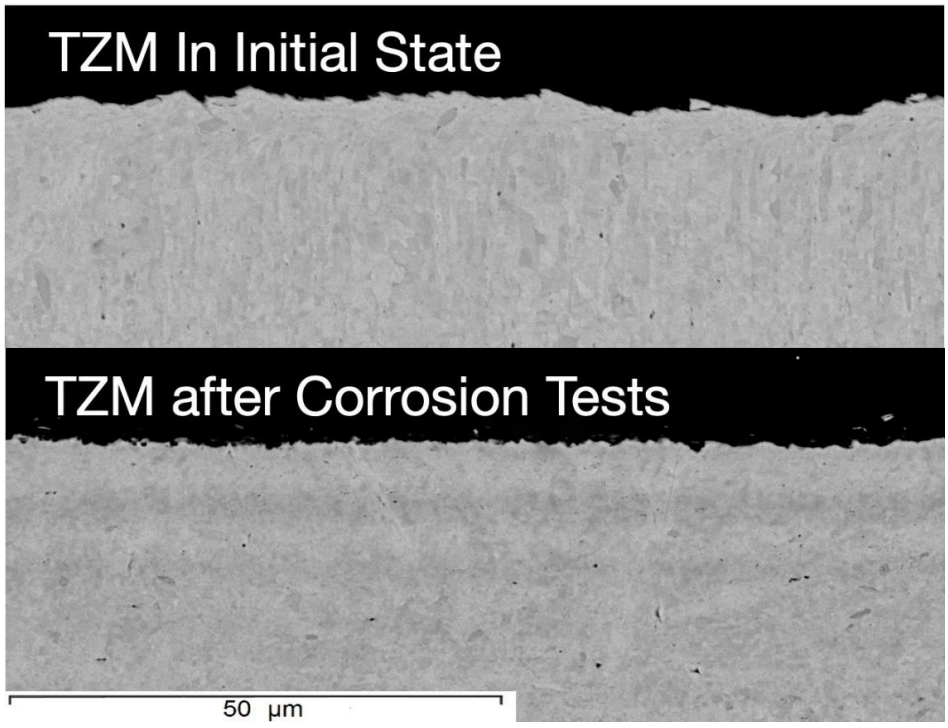


Figure 5. BSE-SEM images of microstructure of TZM alloy samples before and after contact with BLA at 650 °C for 100 h.

Degradation of TZM alloy was caused by selective dissolution of zirconium in bismuth. Chemical analysis of Bi–Li alloys after contact with TZM and literature data (Table 1) support such a conclusion.

The surface of the nickel-based Hastelloy® B-3 alloy showed severe degradation. BSE-SEM images also revealed that the surface of the samples after the corrosion tests was covered by a layer that was different from the bulk of the samples (Figure 6). X-ray microanalysis showed that this layer predominantly consisted of bismuth with dispersed particles of the bulk alloy from which all nickel was dissolved (Figure 7). The mechanism of corrosion of nickel alloys in BLA was described previously [6]. Nickel–molybdenum alloy Hastelloy® B-3, having high molybdenum content (over 28 wt. %), was not an exception. This alloy also showed high corrosion rates due to the dissolution of nickel in bismuth. This process is accompanied by the destruction of the sample's surface and formation of fine molybdenum particles that are easily etched from the surface layer during contact with liquid Bi–Li alloy.

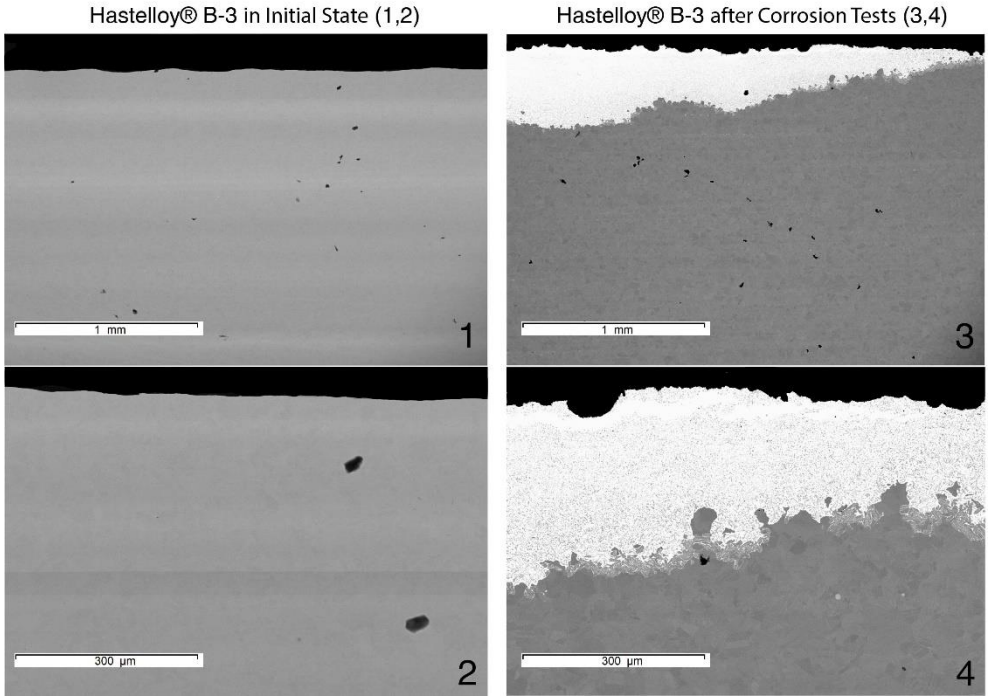


Figure 6. BSE-SEM images of microstructure of Hastelloy® B-3 Alloy samples before and after contact with BLA at 650 °C for 100 h.

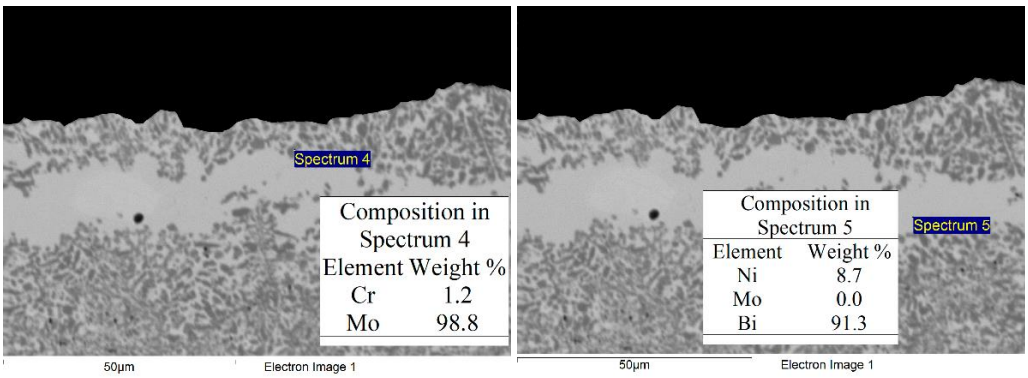


Figure 7. Composition of the surface layer of Hastelloy® B-3 Alloy samples after 100 h contact with Bi–Li (5 mol.%) alloy at 650 °C.

After contact with Bi–Li alloy, nickel-based alloy samples underwent significant structural changes, which resulted primarily from the high solubility of nickel in liquid bismuth. Bismuth selectively leached nickel from the alloys. Molybdenum did not dissolve in bismuth and formed separate alloy particles enriched in molybdenum (Figure 7). It is likely that the leaching of nickel initially resulted in the formation of pores that were subsequently filled by bismuth. As a result, samples of Hastelloy® B-3 alloy after the corrosion tests had a multiphase structure on the surface consisting of zones with high molybdenum content with essentially no nickel present and zones of a new bismuth–nickel alloy. As a result, samples of the nickel-based alloy underwent considerable degradation, and these alloys, therefore, cannot be used as construction materials capable of working in contact with bismuth-containing liquid metal media.

4. Conclusions

The corrosion behavior of several metallic materials in contact with liquid Bi–Li (5 mol.%) alloy was studied. The experiments were carried out under identical conditions for all samples (650 °C, 100 h). Several experimental techniques (SEM/EDS, XRF, and ICP–AES) were used to determine the mechanisms of materials' interaction with molten Bi–Li alloy.

It was confirmed that physical dissolution of metallic samples in liquid metals was the main mechanism of the corrosion. Due to the low solubility of molybdenum and tungsten in liquid bismuth, MoW10, MoW30, and TZM did not significantly corrode in Bi–Li liquid alloy. The corrosion rates were ca. 16 μm/year for MoW10 and MoW30 alloys, and ca. 23 μm/year for TZM. The surface of the samples of these alloys showed uniform corrosion.

Nickel-based alloys showed unsatisfactory corrosion resistance in liquid Bi–Li alloys. Degradation of Hastelloy® B-3 alloy was caused by the etching of nickel by liquid bismuth. Molybdenum, the second main constituent of the alloy, has low solubility in bismuth and formed separate particles surrounded by bismuth–nickel alloy in the surface layer of the material.

Author Contributions: Conceptualization, I.B.P. and V.A.V.; methodology, A.V.A.; software, A.Y.Z.; validation, R.R.A. and A.V.A.; formal analysis, A.Y.Z. and A.V.A.; investigation, R.R.A. and A.I.T.; resources, I.B.P.; data curation, I.B.P.; writing—original draft preparation, A.V.A.; writing—review and editing, I.B.P. and V.A.V.; visualization, S.V.B.; supervision, I.B.P.; project administration, I.B.P. and S.V.B.; funding acquisition, I.B.P. All authors have read and agreed to the published version of the manuscript.

Funding: This study was financially supported by the JSC "Science and Innovations" and JSC RIAR. The research funding from the Ministry of Science and Higher Education of the Russian Federation (Ural Federal University Program of Development within the Priority-2030 Program) is gratefully acknowledged.

Institutional Review Board Statement: Not applicable.

Informed Consent Statement: Not applicable.

Data Availability Statement: The data are available upon request from the corresponding author.

Conflicts of Interest: The authors declare no conflict of interest.

References

1. Kelly, J.E. Generation IV International Forum: A decade of progress through international cooperation. *Prog. Nucl. Energy* **2014**, *77*, 240–246. [CrossRef]
2. International Atomic Energy Agency. *Spent Fuel Reprocessing Options*; IAEA-TECDOC-CD-1587; IAEA: Vienna, Austria, 2009.
3. Ilinčev, G. Research results on the corrosion effects of liquid heavy metals Pb, Bi and Pb–Bi on structural materials with and without corrosion inhibitors. *Nucl. Eng. Des.* **2002**, *217*, 167–177. [CrossRef]
4. Stott, F.H. The protective action of oxide scales in gaseous environments at high temperature. *Rep. Prog. Phys.* **1987**, *50*, 861. [CrossRef]
5. Kofstad, P. *High Temperature Corrosion*; Elsevier Applied Science Publishers, Ltd: Amsterdam, The Netherlands, 1987; p. 413.

6. Abramov, A.V.; Alimgulov, R.R.; Trubcheninova, A.I.; Zhilyakov, A.Y.; Belikov, S.V.; Volkovich, V.A.; Polovov, I.B. Corrosion of Metals and Nickel-Based Alloys in Liquid Bismuth–Lithium Alloy. *Metals* **2021**, *11*, 791. [CrossRef]
7. Rivai, A.K.; Takahashi, M. Compatibility of surface-coated steels, refractory metals and ceramics to high temperature lead-bismuth eutectic. *Prog. Nucl. Energy* **2008**, *50*, 560–566. [CrossRef]
8. Xiao, Z.; Liu, J.; Jiang, Z.; Luo, L. Corrosion behavior of refractory metals in liquid lead at 1000 °C for 1000 h. *Nucl. Eng. Technol.* **2022**, *54*, 1954–1961. [CrossRef]
9. Balandin, Y.F.; Markov, V.G. *Structural Materials for Installations with Liquid Metal Heat Carriers*; Sudpromgiz: Leningrad, Russia, 1961.
10. Okamoto, H.; Schlesinger, M.E.; Mueller, E.M. (Eds.) Bi (Bismuth) Binary Alloy Phase Diagrams, Alloy Phase Diagrams. In *ASM Handbook*; ASM International: Materials Park, OH, USA, 2016; Volume 3, pp. 201–217.
11. Lyakisheva, N.P. (Ed.) *State Diagrams of Double Metal Systems: Handbook*; Elseiver Ltd.: Amsterdam, The Netherlands, 1996; Volume 1.
12. Garg, S.P.; Krishnamurthy, N. The Bi-Ta (bismuth-tantalum) system. *JPE* **1992**, *13*, 269–270. [CrossRef]
13. Polovov, I.B.; Abramov, A.V.; Gibadullina, A.F.; Alimgulov, R.R.; Karpov, V.V.; Zhilyakov, A.Y.; Khotinov, V.A. The effect of microstructure on the corrosion resistance of VDM® alloy C-4 in molten salts. *J. Alloy Compd.* **2019**, *810*, 151758. [CrossRef]
14. Kieffer, R.; Windisch, S.; Nowotny, H. Niobium–Tantalum Infiltrated Alloys. *Metall* **1963**, *17*, 669–677.
15. Brewer, L.; Lamoreaux, R.H. *Molybdenum, Physico-chemical Properties of its Compounds and Alloys*; Atomic Energy Review; Special Issue No.7; IAEB: Vienna, Austria, 1980.
16. Baren, M.R. The Ag-Mo (silver-molybdenum) system. *Bull. Alloy Phase Diagr.* **1990**, *11*, 548–549. [CrossRef]
17. Reed, E.L. Stability of Refractories in Liquid Metals. *J. Am. Ceram. Soc.* **1954**, *37*, 146–152. [CrossRef]

Disclaimer/Publisher's Note: The statements, opinions and data contained in all publications are solely those of the individual author(s) and contributor(s) and not of MDPI and/or the editor(s). MDPI and/or the editor(s) disclaim responsibility for any injury to people or property resulting from any ideas, methods, instructions or products referred to in the content.